A NOVEL COMPRESSIVE SENSING APPROACH TO SIMULTANEOUSLY ACQUIRE COLOR AND NEAR-INFRARED IMAGES ON A SINGLE SENSOR

Zahra Sadeghipoor[1], Yue M. Lu[2], and Sabine Süsstrunk[1]

[1]School of Computer and Communication Sciences
École Polytechnique Fédérale de Lausanne (EPFL), Lausanne, Switzerland
[2] Harvard School of Engineering and Applied Sciences, Cambridge, MA 02138, USA

ABSTRACT

Sensors of most digital cameras are made of silicon that is inherently sensitive to both the visible and near-infrared parts of the electromagnetic spectrum. In this paper, we address the problem of color and NIR joint acquisition. We propose a framework for the joint acquisition that uses only a single silicon sensor and a slightly modified version of the Bayer color-filter array that is already mounted in most color cameras. Implementing such a design for an RGB and NIR joint acquisition system requires minor changes to the hardware of commercial color cameras.

One of the important differences between this design and the conventional color camera is the post-processing applied to the captured values to reconstruct full resolution images. By using a CFA similar to Bayer, the sensor records a mixture of NIR and one color channel in each pixel. In this case, separating NIR and color channels in different pixels is equivalent to solving an under-determined system of linear equations. To solve this problem, we propose a novel algorithm that uses the tools developed in the field of compressive sensing. Our method results in high-quality RGB and NIR images (the average PSNR of more than 30 dB for the reconstructed images) and shows a promising path towards RGB and NIR cameras.

Index Terms— Color filter array, demosaicing, the Bayer CFA, near-infrared, compressive sensing, sparse decomposition.

1. INTRODUCTION

Near-infrared (NIR) is a part of the electromagnetic spectrum with an approximate wavelength range of 700 nm to 1100 nm. Silicon, the light-sensitive material of sensors in most color cameras, is sensitive to the NIR band, as well as the visible part of the spectrum. In a digital camera, an interference filter, called hot-mirror, usually blocks the NIR. It has recently been shown, however, that retaining, instead of removing, the additional information offered by NIR and combining them with the visible representation of the scene improves the performance of several tasks in computer vision and computational photography, including semantic segmentation [1], skin smoothing [2], image enhancement [3, 4], and video conference relighting [5]. All of these applications need RGB (red, green, and blue) and NIR channels of the scene. In the following, we call these four-channel images RGBN.

In most color cameras, only one single sensor is used to capture three channels (red, green, and blue). A color-filter array (CFA) spatially samples color channels and results in a one-channel image

called the "mosaiced" image. One of the most commonly used CFAs in current color cameras is the Bayer CFA [6] (see Fig. 1-a). After acquisition, to reconstruct the full-resolution color image, an interpolation algorithm, referred to as "demosaicing", is applied to the mosaiced image.

It is possible to design a camera that simultaneously captures RGB and NIR images using the same schematic implemented in color imaging. The two main design issues in such a camera are CFA and demosaicing.

Lu *et al.* in [7] propose an algorithm that optimizes the CFA and demosaicing for the RGBN camera. In [7], the authors assume that each pixel of the CFA transmits a linear combination of three color channels and NIR. The optimum coefficients for the linear combination in every pixel and the demosaicing matrix are computed by solving an optimization problem that minimizes the demosaicing error. However, implementing their proposed CFA, instead of the ones usually used in color cameras, requires hardware changes (see Fig. 1-b).

To eliminate additional manufacturing costs for changing the hardware, in this paper we propose to use a CFA similar to Bayer in the RGBN camera. The only difference between our proposed CFA and the original Bayer is that the two green filters in our CFA have different transmittances. Here, transmittance means the amount of light the filter transmits in the given wavelength range. We will explain our motivation for this modification in Section 2. By using a similar CFA for acquisition of RGBN images, one of the very few hardware modifications needed to change a conventional color camera to an RGBN one is to remove the hot-mirror.

Without the hot-mirror filter, a mixture of one color channel and NIR is captured at each spatial position on the sensor [1]. Hence, to have full resolution NIR and RGB images, we first need to separate the NIR and color channels in different pixels of the mosaiced image. Our main contribution in this paper is to propose an algorithm that separates these signals by exploiting their spatial and spectral correlations. Once the color and NIR channels are successfully separated, the NIR intensities are known in all pixels, but the intensities of two color channels are missing in each pixel. Reconstructing the full resolution RGB image, however, is the conventional color demosaicing problem with numerous solutions available (for a few examples see [8, 9, 10, 11]).

In our problem, only one measurement is available at every pixel and two unknowns need to be approximated. Therefore, it is equivalent to an under-determined system of equations and does not have a unique solution unless we impose some additional constraints on the unknown signals. Our target signals are color and NIR images

[1]Note that the filters in the Bayer CFA do not block NIR. See Fig. 1-c.

of natural scenes, which exhibit strong spatial and spectral correlations. As a result, these images can be *sparsely* represented in a de-correlating transform domain. Thus, a small number of measurements can be used to approximate the sparse transform coefficients of these signals. Once the coefficients are approximated, the unknown signals are computed by the inverse transform.

The success of our algorithm depends on how sparse the target signals can be represented in the transform domain. We are not aware of any existing transform that is specifically designed to sparsify RGB and NIR images. In this paper, we propose using a cascade of two transforms to sparsely represent these images. One of these transforms exploits the spatial correlation and the other one decorrelates RGBN images spectrally. This transform is explained in more details in Section 2.

The task of separating color channels and NIR is similar to the problem of interest in the field of compressed sensing [12], where a few measurements are used to approximate a high-dimensional signal. The main difference between most of the studies in this field and our work is in the measurement step. In compressive sensing, usually every measurement is a random linear combination of all samples in the signal. Thus, the measurement matrix that maps the signal to measurements is a fully random matrix. However, in our application because of the limitations imposed by hardware, it is not possible to have a fully random measurement matrix. To cope with this issue, we propose a new measurement matrix in Section 2.

Our proposed algorithm shows promising performance in the joint acquisition of RGBN images. In Section 3, we compare the performance of our algorithm with the one proposed in [7]. We conclude the paper in Section 4.

1.1. Related Work

There are several studies that use compressive sensing tools in the acquisition of color and multispectral images. In [13], Golbabaee and Vandergheynst address the problem of reconstructing hyperspectral images from a few noisy measurements. The main difference between their work and ours is that they are mostly interested in remote sensing images, hence they assume that there are only a small number of materials present in every scene. However, our target images are those taken in everyday photography and the main assumption of [13] no longer holds for these images.

Nagesh and Li in [14], and Majumdar and Ward in [15] propose two different frameworks for the compressed acquisition of color images. In these studies, the assumption is that the sensor measures a linear combination of the whole image in every pixel, which requires a major alteration in the hardware of current cameras.

The compressive acquisition and demosaicing of color images are also studied in [16] and [17]. In both of these papers, the authors propose using a CFA that transmits a linear combination of all color channels in every pixel. Our work is significantly different from [16, 17], because our goal is to capture four channels instead of three, and we use only a modified Bayer CFA.

2. THE PROPOSED ALGORITHM

By using a single silicon sensor, a mixture of NIR and one color channel is stored in each pixel of the mosaiced image (see Fig. 1-a).

To estimate the full resolution RGB and NIR images, we first un-mix the green and NIR channels in odd rows and columns, and even rows and columns of the mosaiced image. Since in the Bayer CFA the green sampling rate is twice that of red and blue, separating green and NIR can be done with higher accuracy. We then interpolate the NIR pixel intensities computed in this step to estimate the
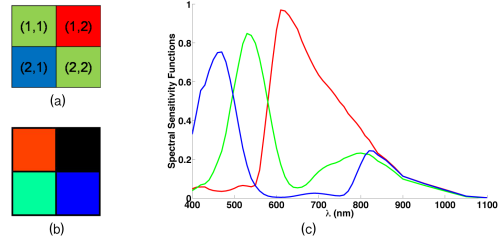

Fig. 1. (a) The Bayer CFA. This figure also shows the spatial arrangement of colors in the mosaiced image (indices in each pixel indicate the number of the corresponding row and column). (b) The 2×2 CFA optimized by the algorithm of [7]. The black pixel transmits only NIR. (c) Spectral sensitivities of red, green, and blue pixels in a commercial color camera without hot-mirror.
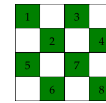

Fig. 2. A block of size 4×4 in the mosaiced image. Green pixels contain a mixture of green and NIR. Indices in these pixels show how we arrange the measurements in $\boldsymbol{y}$ (see equation (1)).

full resolution NIR image.

The estimated NIR intensities in odd (or even) rows and even (or odd) columns are used to compute red (or blue) values in corresponding pixels. At this step the color image is still mosaiced. Estimating the missing color information, however, is simply the conventional problem of color demosaicing when the Bayer CFA is used to sample the color channels, and can be solved with any existing color demosaicing algorithm.

2.1. Green and NIR Separation

In this subsection, we first introduce some notations, and then mathematically formulate the problem of separating green and NIR channels. We will then continue with a detailed description of the algorithm proposed to solve this problem.

2.1.1. Problem Statement

Let us consider a block of size $\sqrt{n} \times \sqrt{n}$ in the mosaiced image (see Fig. 1-a for an illustration). In such a block, $\frac{n}{2}$ pixels contain a mixture of green and NIR intensities [2]. We call the measurement (mixture of green and NIR) in the ith pixel of the block y_i. Consequently, all green and NIR mixtures in this block can be written in the following vector form:

$$\boldsymbol{y} = [y_1, y_2, \cdots, y_m]^T, \qquad m = \frac{n}{2}. \qquad (1)$$

Note that the measurements are arranged in the vector $\boldsymbol{y}$ such that the values captured by one period of the 2×2 CFA are placed adjacent to each other (indices in Fig. 2 show this arrangement).

The unknowns in this problem are green and NIR intensities in the corresponding pixels. These values form the following vector:

$$\boldsymbol{x} = [G_1, G_2, \cdots, G_m, N_1, N_2, \cdots, N_m], \qquad (2)$$

---

[2]Here, for the sake of simplicity, we assume that n is an even number. All the equations can be used in the case of n being an odd number with minor modifications.

where G_i and N_i are, respectively, green and NIR intensities in pixel i. It is important to note that the order of pixels in $\boldsymbol{x}$ is exactly the same as pixel arrangements in $\boldsymbol{y}$ (see equation (1)).

As every measurement is a linear combination of green and NIR, vector $\boldsymbol{x}$ (unknowns) and $\boldsymbol{y}$ (measurements) are related through the following matrix multiplication:

$$\boldsymbol{y}^{m \times 1} = \boldsymbol{M}^{m \times n} \times \boldsymbol{x}^{n \times 1}, \qquad m = \frac{n}{2}, \qquad (3)$$

where $\boldsymbol{M}$ is the measurement matrix defined by the CFA. In the above equation, superscripts specify the dimensions of the corresponding matrix and vectors.

Assuming that the Bayer CFA is used to sample the scene, we can write the matrix $\boldsymbol{M}$ as follows:

$$\boldsymbol{M}^{m \times n} = [\boldsymbol{M_G}^{m \times m}, \boldsymbol{M_N}^{m \times m}], \qquad (4)$$

where

$$
\boldsymbol{M_G} = \begin{bmatrix} \alpha_1 & 0 & 0 & \cdots & 0 \\ 0 & \alpha_2 & 0 & \cdots & 0 \\ 0 & 0 & \alpha_1 & 0 & \cdots \\ \vdots & & & & \end{bmatrix},
$$

$$
\boldsymbol{M_N} = \begin{bmatrix} \beta_1 & 0 & 0 & \cdots & 0 \\ 0 & \beta_2 & 0 & \cdots & 0 \\ 0 & 0 & \beta_1 & 0 & \cdots \\ \vdots & & & & \end{bmatrix}. \qquad (5)
$$

In $\boldsymbol{M_G}$ and $\boldsymbol{M_N}$, α_1 and β_1 are, respectively, the relative sensitivities of the first green filter in the CFA to green (α_1) and to NIR (β_1). Similarly, α_2 and β_2 are the sensitivities of the second filter to green and NIR. To have physically realizable filters, these coefficients should satisfy the following conditions:

$$
\begin{aligned}
& 0 < \alpha_1, \alpha_2, \beta_1, \beta_2 < 1 \\
& \alpha_1 + \beta_1 = 1, \alpha_2 + \beta_2 = 1.
\end{aligned} \qquad (6)
$$

Using the notations introduced so far, the problem of un-mixing green and NIR translates to finding vector $\boldsymbol{x}$, knowing $\boldsymbol{y}$ and $\boldsymbol{M}$. As mentioned above, this problem is an under-determined system of linear equations (USLE) and has a unique solution only if some constraints are imposed on the green and NIR channels. One of the most accepted assumptions about natural images is the smoothness of these signals, which results in a sparsity of their coefficients in some transform domains, such as DCT or wavelet transform. In this paper, we impose the same constraint on green and NIR channels and assume that these signals are sparse in some transform domain, called $\boldsymbol{\Phi}$. Thus, in the following equation:

$$\boldsymbol{x} = \boldsymbol{\Phi s}, \qquad (7)$$

where $\boldsymbol{s}$ contains the coefficients of $\boldsymbol{x}$ in the transform domain ($\boldsymbol{\Phi}$), $\boldsymbol{s}$ is likely to be sparse.

By imposing the sparsity constraint, the task of separating these channels can be accomplished by solving the following optimization problem:

$$\boldsymbol{s}^\star = \operatorname{argmin} \|\boldsymbol{s}\|_0, \qquad \text{subject to} \quad \boldsymbol{y} = \boldsymbol{Mx} = \boldsymbol{M\Phi s}. \qquad (8)$$

Here, $\|.\|_0$ is the quasi l_0 norm, which is the number of non-zero elements in a vector (a measure of sparsity).

The above optimization problem (or its ℓ_1 relaxation) can be solved by any sparse decomposition algorithm such as orthogonal matching pursuit (OMP) [18], basis pursuit (BP) [19], or smoothed l_0 (SL0) [20]. After solving (8), we can compute green and NIR pixel intensities as $\boldsymbol{x} = \boldsymbol{\Phi s}^\star$.

2.1.2. The Measurement Matrix ($\boldsymbol{M}$)

As explained in 2.1.1, the structure of the measurement matrix ($\boldsymbol{M}$) in our application is determined by the CFA. We assume that the RGBN camera uses the Bayer CFA, thus the structure of the measurement matrix is in the form of (4) and (5).

In the field of compressed sensing, the restricted isometry property (RIP) of the measurement matrix has been shown to be a sufficient condition to guarantee the perfect recovery of a sparse signal from an under-determined set of linear measurements [21]. Furthermore, it has been shown that random matrices with i.i.d entries fulfil the RIP condition with high probability [21]. As such, random matrices are among the most used measurement matrices in compressed sensing.

To have a measurement matrix as similar as possible to the fully random matrix, we propose to *randomly* choose α_1 and α_2 in $\boldsymbol{M}$ (see (5)). This means that we need to change the transmittances of two green filters of the CFA in the NIR and green spectral bands. Yet, because of the constraints imposed by hardware (the structure of CFA), our measurement matrix is far from being ideal. However, our experiments show that even the sparse random matrix proposed in this paper leads to promising results in our specific application.

According to the Lambert-Beer law, the transmittance of an optical filter can be controlled by adjusting its thickness and changing the wavelength of the incident light [22]:

$$T(z) = e^{-\alpha z}, \qquad (9)$$

where T is the relative transmittance, z is the filter thickness and α is its absorption constant that changes with the wavelength. As a result, it is feasible to place two green filters with different and predefined transmittances in green and also NIR bands. Note that once we choose the filter transmittances randomly, they are fixed and will be used for all images.

2.1.3. Sparsifying Transform ($\boldsymbol{\Phi}$)

The success of the separation algorithm proposed in this paper highly depends on how sparse the target signal is in the transform domain ($\boldsymbol{\Phi}$).

As de-correlating transforms usually result in sparse representations of the signal, we use a de-correlating transform as $\boldsymbol{\Phi}$. In our problem, the target signal ($\boldsymbol{x}$ in (2)) is the concatenation of green and NIR pixel intensities in a small neighborhood. Since vector $\boldsymbol{x}$ contains neighboring green (and also NIR) intensities, the data is *spatially* correlated. Moreover, as it represents part of the scene in two spectral bands, strong *spectral* correlation is present in our target signal.

Therefore, we propose to use a cascade of two different transforms as $\boldsymbol{\Phi}$. One of these transforms explores spatial correlations in the data. To spatially sparsify green and NIR channels, we use the following matrix:

$$\boldsymbol{D}_{\text{spatial}} = \boldsymbol{I}_{2 \times 2} \otimes \boldsymbol{D}_{\text{DCT}} \qquad (10)$$

where $\boldsymbol{D}_{\text{DCT}}$ is the DCT transform matrix, $\boldsymbol{I}_{2 \times 2}$ is the identity matrix of size 2×2, and $\otimes$ denotes the Kronecker product.

To spectrally decorrelate the signal, we propose to use the transform derived from principal components analysis (PCA) of the green and NIR channels. To summarize, the sparsifying transform can be written as follows:

$$\boldsymbol{\Phi} = \boldsymbol{D}_{\text{PCA}} \times \boldsymbol{D}_{\text{spatial}}, \qquad (11)$$

	Optimum CFA	Our algorithm
CPSNR	31.44	30.28
PSNR	37.12	33.26

Table 1. The results of the optimum CFA algorithm [7] and our method. This table shows the average CPSNR (for color images) and PSNR (for NIR images) for 20 pairs of images.

where D_{PCA} transforms the data to the principal components space.

To represent the target signal even more sparsely, we update our proposed transform (11) using the K-SVD dictionary learning algorithm presented by Aharon *et al.* [23]. This algorithm trains a transformation in a manner that it can represent training signals as sparse as possible with a user-defined accuracy.

2.2. Red (Blue) and NIR Separation

Un-mixing red (blue) and NIR channels in odd (even) rows and even (odd) columns of the image can be done with the approach proposed in Section 2.1. However, notice that the sampling rate of red and blue channels in the Bayer CFA is half of the green sampling rate. Thus, the red measurements in one block are not spatially correlated as strongly as the green and NIR mixtures are in the same block. As a result, un-mixing red (blue) and NIR channels is much more challenging. Our experiments confirms that solving (8) to separate red (blue) and NIR does not lead to high accuracy approximations.

To solve this issue, we interpolate the NIR intensities computed in the previous step (un-mixing green and NIR) to obtain the full resolution NIR image. Then, red or blue pixel intensities can be easily computed by subtracting the NIR intensities from sensor measurements in the corresponding pixels.

Recall that to separate green and NIR channels, the transmittances of green filters in the CFA have to be chosen randomly. However, we do not use (8) to un-mix red (blue) and NIR. Thus, red and blue filters of our proposed CFA are exactly the same as the filters currently placed on the Bayer CFA.

3. SIMULATION RESULTS

In this section, we evaluate the performance of our algorithm in the joint acquisition of RGB and NIR images by using a single sensor and the modified Bayer CFA. We compare the results of our algorithm with the method proposed in [7] that uses an optimized CFA and linear demosaicing for RGBN joint acquisition.

For both algorithms, we use 40 pairs of RGBN images (size of 512×768 pixels) as the training set. In our method the transformation matrix (Φ), and in the optimum CFA algorithm the CFA and the demosaicing matrix are learned from the training set. We use the SL0 sparse decomposition algorithm [20] in the separation step of our framework. To interpolate the NIR image, we use a simple bilinear interpolation and color images are demosaiced with the algorithm presented in [9].

α_1 and α_2 in the measurement matrix (see equation (5)) are uniform random coefficients, and β_1 and β_2 are computed using (6). We empirically found out that the transmittances of two green filters in green (and also in NIR) should differ by more than a certain threshold in order for the sparse decomposition algorithm to converge with our specific measurement matrix. Our experiments show that a difference of about 30% guarantees the success of the algorithm. Deriving precise constraints for the measurement matrix requires analyzing the convergence of the algorithm, which is part of
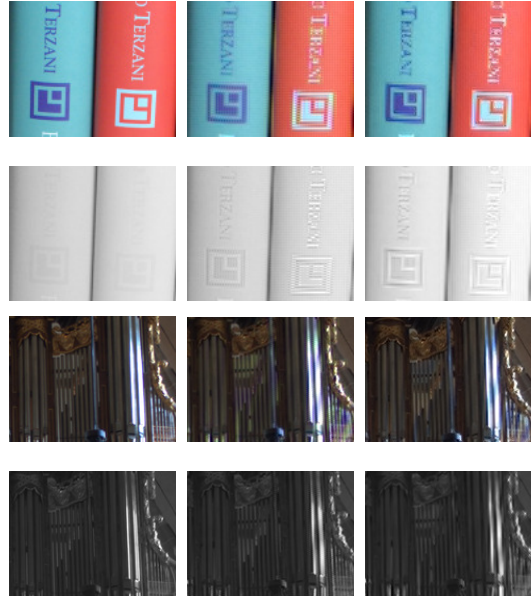

Fig. 3. RGB and NIR images reconstructed by the optimum CFA method and our algorithm. From left to right: crop of the original image, the results of the optimum CFA algorithm and our method. First and third rows: RGB images, second and fourth rows: NIR images.

our future work.

Table 1 summarizes the average color peak signal-to-noise ratio (CPSNR) for RGB images and peak signal-to-noise ratio (PSNR) of NIR for 20 pairs of test images (each with 512×768 pixels).

Note that the optimum CFA algorithm optimizes 12 coefficients for a CFA of size 2×2 (3 color coefficients in each pixel). Whereas, our algorithm needs only four different coefficients (two in each of the green filters). Despite this fact, the quality of RGB images reconstructed by our algorithm is more or less similar to the results of the optimum CFA. However, the optimum CFA method is more successful in demosaicing NIR images. The reason is that in the CFA optimized by this algorithm, one out of four filters transmits only NIR (see Fig. 1-b). However, implementing a filter that transmits only NIR and blocks visible with a sharp cutoff is usually more difficult than producing filters with different transmittances (or thicknesses).

To visually compare the results of the optimum CFA and our algorithm, we show small regions of RGB and NIR images reconstructed by both algorithms in Figure 3.

4. CONCLUSION

We have proposed using a single silicon sensor and a modified Bayer CFA for the joint acquisition of RGB and NIR images. We have presented a novel algorithm that un-mixes NIR and green channels in this setup using tools from compressed sensing. Once the separation step is performed, full resolution NIR and RGB images are estimated by conventional image interpolation and color demosaicing algorithms. Simulation results show that our proposed algorithm leads to high visual quality in the reconstructed RGBN images.

5. REFERENCES

[1] N. Salamati, D. Larlus, G. Csurka, and S. Süsstrunk, "Semantic image segmentation using visible and near-infrared channels," in *ECCV Workshop on Color and Photometry*, 2012.

[2] C. Fredembach, N. Barbuscia, and S. Süsstrunk, "Combining visible and near-infrared images for realistic skin smoothing," in *IS&T/SID 17th Color Imaging Conference (CIC)*, 2009.

[3] D. Krishnan and R. Fergus, "Dark flash photography," *ACM Transactions on Graphics*, vol. 28, no. 3, pp. 1–11, 2009.

[4] S. Süsstrunk and C. Fredembach, "Enhancing the visible with the invisible: exploiting near-infrared to advance computational photography and computer vision," in *SID International Symposium Digest*, 2010.

[5] P. Gunawardane, T. Malzbender, R. Samadani, A. McReynolds, D. Gelb, and J. Davis, "Invisible light : Using infrared for video conference relighting," in *IEEE International Conference on Image Processing (ICIP)*, 2010.

[6] B. E. Bayer, "Color imaging array," 1976, U.S. Patent 3971065.

[7] Y. M. Lu, C. Fredembach, M. Vetterli, and S. Süsstrunk, "Designing color filter arrays for the joint capture of visible and near-infrared images," in *IEEE International Conference on Image Processing (ICIP)*, 2009.

[8] X. Li, "Demosaicing by successive approximation," *IEEE Transactions on Image Processing*, vol. 14, no. 3, pp. 370–379, 2005.

[9] K. Hirakawa and T. W. Parks, "Adaptive homogeneity-directed demosaicing algorithm," *IEEE Transactions on Image Processing*, vol. 14, no. 3, pp. 360–369, 2005.

[10] B. K. Gunturk, Y. Altunbasak, and R. M. Mersereau, "Color plane interpolation using alternating projections," *IEEE Transactions on Image Processing*, vol. 11, no. 9, pp. 997–1013, 2002.

[11] D. Alleysson, S. Süsstrunk, and J. Hérault, "Linear demosaicing inspired by the human visual system," *IEEE Transactions on Image Processing*, vol. 14, no. 4, pp. 439–449, 2005.

[12] D. L. Donoho, "Compressed sensing," *IEEE Transactions on Information Theory*, vol. 52, no. 4, pp. 1289–1306, 2006.

[13] M. Golbabaee and P. Vandergheynst, "Hyperspectral image compressed sensing via low-rank and joint-sparse matrix recovery," in *IEEE International Conference on Acoustics, Speech, and Signal Processing (ICASSP)*, 2012.

[14] P. Nagesh and B. Li, "Compressive imaging of color images," in *IEEE International Conference on Acoustics, Speech, and Signal Processing (ICASSP)*, 2009.

[15] A. Majumdar and R. K. Ward, "Compressed sensing of color images," *Elsevier Signal Processing*, vol. 90, no. 12, pp. 3122–3127, 2010.

[16] A. A. Moghadam, M. Aghagolzadeh, M. Kumar, and H. Radha, "Compressive demosaicing," in *IEEE International Workshop on Multimedia Signal Processing (MMSP)*, 2010.

[17] M. Aghagolzadeh, A. A. Moghadam, M. Kumar, and H. Radha, "Compressive demosaicing for periodic color filter arrays," in *IEEE International Conference on Image Processing (ICIP)*, 2011.

[18] Y. C. Pati, R. Rezaiifar, and P. S. Krishnaprasad, "Orthogonal matching pursuit: Recursive function approximation with applications to wavelet decomposition," in *27th Annual Asilomar Conference on Signals, Systems, and Computers*, 1993.

[19] S. S. Chen, D. L. Donoho, and M. A. Saunders, "Atomic decomposition by basis pursuit," *SIAM Review*, vol. 43, no. 1, pp. 129–159, 2001.

[20] H. Mohimani, M. Babaie-Zadeh, and C. Jutten, "A fast approach for overcomplete sparse decomposition based on smoothed L_0 norm," *IEEE Transactions on Signal Processing*, vol. 57, no. 1, pp. 289–301, 2009.

[21] E. J. Candes and T. Tao, "Near-optimal signal recovery from random projections: Universal encoding strategies?," *IEEE Transactions on Information Theory*, vol. 52, no. 12, pp. 5406–5425, 2006.

[22] H. Gross, *Handbook of Optical Systems, Volume 1, Fundamentals of Technical Optics*, Wiley, 2011.

[23] M. Aharon, M. Elad, and A. M. Bruckstein, "The K-SVD: An algorithm for designing of overcomplete dictionaries for sparse representation," *IEEE Transactions on Signal Processing*, vol. 54, no. 11, pp. 4311–4322, 2006.